RESEARCH PAPER

Pharmacological Characterization of a Substituted Pyrrolizidine Derivative as a Dual Inhibitor of JAK1 Kinase and Pseudokinase Domains in Hepatocellular Carcinoma.

Supritha G Swamy[1], Vijay Ramesh[2], Meghashree Gangatikar[2], Sathyamurthy Srinivasa[2], Babu Shubha Priya[3], Ranjith Siddaraju[3], Chandan Shivamallu[4], Hema B. P[1], Bhargav Shreevatsa[2*], Nanjunda Swamy Shivananju[1*]

[1]*Department of Biotechnology, JSS Science and Technology University, Sri Jayachamarajendra College of Engineering, JSS Technical Institutions Campus, Mysuru- 570006, Karnataka, India*
[2]*Department of Microbiology, JSS Academy of Higher Education and Research, Mysuru, 570015*
[3]*Department of Studies in Chemistry, University of Mysore, Manasagangotri, Mysuru-570006, Karnataka India.*
[4]*Department of Biotechnology and Bioinformatics, JSS Academy of Higher Education and Research, Mysuru-570015*

ABSTRACT
Hepatocellular carcinoma (HCC) remains one of the most prevalent and lethal malignancies worldwide, with limited therapeutic options and a poor prognosis. In the present study, a substituted pyrrolizidine derivative was computationally evaluated for its inhibitory potential against Janus kinase 1 (JAK1), a critical mediator of oncogenic signalling in HCC. The structural integrity of the JAK1 kinase of PDB ID: 4EI4 and the pseudokinase of PDB ID: 4L01 domains was validated through Ramachandran plot analysis, confirming over 99% of residues within energetically favourable regions. Molecular docking was performed using the Schrödinger Glide module under standard and extra precision modes to predict ligand binding affinity and interaction stability. The pyrrolizidine derivative exhibited a markedly higher affinity toward the catalytic kinase domain, reflected by a docking score of –11.0 kcal/mol, compared with –8.4 kcal/mol for the pseudokinase domain. Multiple hydrogen bonds and hydrophobic interactions within the ATP-binding cleft were observed, indicating stable and specific ligand–protein engagement. Molecular dynamics simulations further confirmed complex stability throughout a 100 ns trajectory. These findings suggest that the pyrrolizidine derivative acts as a selective JAK1 inhibitor capable of modulating aberrant signalling pathways associated with HCC progression. Further in vitro and in vivo validation is warranted to confirm its therapeutic potential and safety profile. The study highlights the promise of pyrrolizidine-based scaffolds as rationally designed candidates for next-generation JAK1-targeted therapeutics in liver cancer management.

Keywords: Hepatocarcinoma Cellular Carcinoma (HCC), JAK protein, Pyrrolizidine, Molecular dynamic simulations.
How to cite this article: Swamy SG, Ramesh V, Gangatikar M, Srinivasa S, Priya BS, Siddaraju R, Shivamallu C, P HB, Shreevatsa B, Shivananju NS, Pharmacological Characterization of a Substituted Pyrrolizidine Derivative as a Dual Inhibitor of JAK1 Kinase and Pseudokinase Domains in Hepatocellular Carcinoma..Int J Drug Deliv Technol. 2026;16(2s): 465-472; DOI: 10.25258/ijddt.16. 465-472
Source of support: Nil.
Conflict of interest: None

INTRODUCTION

Liver cancer represents one of the most lethal malignancies, ranking third worldwide in cancer-related deaths with 757,948 reported fatalities and sixth in new diagnoses with 865,269 cases documented in 2022 (1). Primary liver cancers mainly consist of hepatocellular carcinoma (HCC) and intrahepatic cholangiocarcinoma, with HCC accounting for nearly 75–85% and cholangiocarcinoma contributing 10–15% of cases (1). Several well-established risk factors are linked to HCC development, including hepatitis B and C viral infections, aflatoxin exposure, excessive alcohol consumption, obesity, smoking, and type 2 diabetes (2). Current clinical interventions involve surgical resection, liver transplantation, radiation therapy, and chemotherapy (3). However, chemotherapeutic agents often display limited success due to the frequent late-stage diagnosis of HCC. This underscores the necessity of identifying novel small molecules that can effectively suppress tumour growth even in advanced disease stages

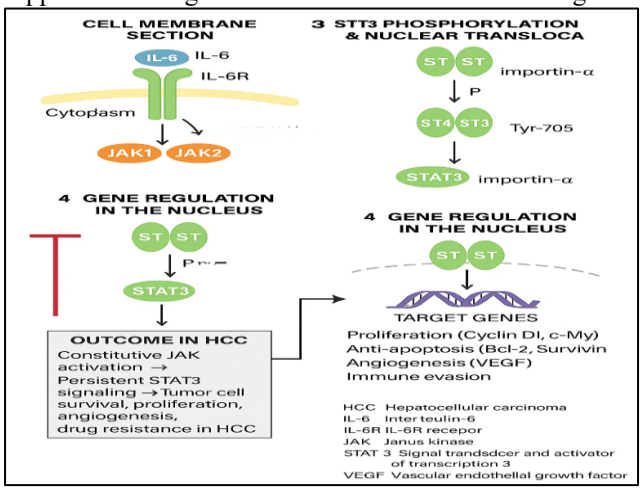

**Author for Correspondence: Bhargav Shreevatsa*

Figure 1. Schematic representation of the IL-6/JAK signalling pathway in hepatocellular carcinoma (HCC). IL-6 binding to IL-6R activates JAK1 kinase, leading to phosphorylation, dimerization, and nuclear translocation. Activated regulates target genes that promote proliferation, anti-apoptosis, angiogenesis, and immune evasion, contributing to tumour survival and drug resistance in HCC

Among the critical proteins implicated in liver cancer progression are members of the Janus kinase (JAK) family. JAKs are non-receptor tyrosine kinases that play a central role in cytokine-mediated signalling and have been found aberrantly activated in a wide spectrum of cancers, including HCC (4, 6). Under normal physiological conditions, JAKs remain inactive until triggered by cytokines such as interleukin-6 (IL-6) binding to their cognate cell-surface receptors (7). This interaction induces conformational changes that activate JAK1, enabling it to phosphorylate downstream signalling proteins on critical tyrosine residues (Figure 1)(8, 9). The activation of these pathways ultimately regulates gene expression programmes that promote cell proliferation, survival, angiogenesis, and immune evasion (10–12). JAK1 is a key mediator of the JAK-1 signalling pathway, which is frequently dysregulated in hepatocellular carcinoma. Aberrant activation leads to uncontrolled cell proliferation, resistance to apoptosis, angiogenesis, and immune evasion. Based on the existing studies, if a desired ligand binds to the ATP-binding pocket of JAK1, it can prevent phosphorylation, effectively shutting down downstream oncogenic signalling cascades. In HCC, blocking JAK1 helps to suppress tumour growth signals, enhance apoptosis, reduce metastatic potential and improve the efficacy of immune checkpoint therapies, since JAK influences immune escape. Targeting the JAK signalling axis has therefore emerged as a promising therapeutic strategy in oncology. Small-molecule inhibitors designed to interfere with JAK activity are being actively investigated to suppress aberrant signalling cascades.

Pyrrolizidine, a fused heterocyclic scaffold containing two five-membered rings with nitrogen as a shared atom, has been highlighted in earlier studies for its anticancer activity in cellular systems (Figure 2) (13–16). Nevertheless, the specific molecular partners and precise mechanisms underlying its activity remain unclear. In this context, we established a pyrrolizidine derivative where the ligand contains aromatic ring systems (highlighted in green), which facilitate π–π stacking interactions with hydrophobic residues inside the ATP-binding pocket of JAK1 (17). This is critical because most kinase inhibitors mimic ATP to block phosphorylation competitively. The nitrogen atoms in heteroaromatic rings (blue) can act as hydrogen bond acceptors/donors, stabilising the ligand inside the catalytic cleft by interacting with amino acids like Lys, Glu, or Asp commonly present in kinase active sites. The tert-butyl substituents (green branched groups) increase lipophilicity, improving membrane permeability, and help anchor the ligand in hydrophobic regions of JAK1's binding site, thereby enhancing selectivity. The oxygen atoms (red), likely present as carbonyl or ether linkages, provide polar interaction points that can strengthen hydrogen bonding with hinge-region residues of JAK1. This hinge binding is crucial for effective kinase inhibition (17).

The presented ligand is structurally optimised for ATP-competitive inhibition of JAK1, making it a promising small-molecule candidate against HCC. Its aromatic scaffolds allow stable docking, while heteroatoms enable critical hydrogen bonding with JAK1 residues. By interfering with the JAK1 axis, this compound could suppress tumour progression and support targeted therapeutic approaches for liver cancer. The current study involves the evaluation of Pyrrolizidine derivatives, with the potential to inhibit JAK1-driven signalling events in HCC models, to identify effective candidates for therapeutic intervention.

MATERIALS AND METHODS

2.1. Ligand Preparation

The 2D structure of the selected ligand was initially drawn using ChemSketch and converted to PDB format and visualised in PyMOL (22). Ligand preparation was performed using the LigPrep module in Schrödinger (23), which generated 3D conformations, optimised geometries, and appropriate ionisation states. The active site for docking was defined by generating a receptor grid using the Sitemap tool, and the lowest energy conformer of the ligand was retained for docking analysis. This ligand is assessed with SwissADME analysis to study the Pharmacokinetic properties of the ligand and its toxic effects, the ADMET studies and analysis graphs are mentioned in Supplementary Figure 6 and Supplementary Figure 7, Supplementary Table 1.

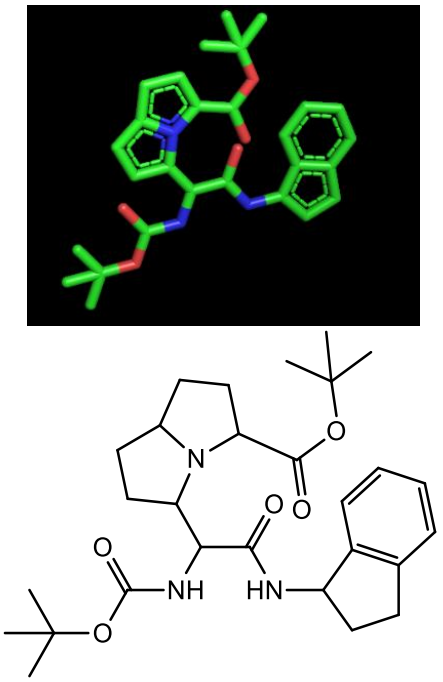

(A) (B)

Figure 4. ***IUPAC Name: 5-[tert-Butyloxycarbonylamino-(indan-1yl-hexahydro-pyrrolizine-3-carboxylicacid tert-butyl ester. (A) 2D, (B)*** **Three-dimensional structure of the synthesised ligand.**

2.2. Protein Preparation

The crystal structure of Janus kinase 1 (JAK1) (PDB ID: 4EI4, resolution of 1.64 Å) and pseudo kinase 1 (PDB ID: 4L01, resolution of 1.90 Å**)** was retrieved from the Protein Data Bank (Figure 2). Protein preparation was performed using the Protein Preparation Wizard in Pymol *Version 3.1.3* (24). Solvent molecules and crystallographic water molecules were removed, bond orders were assigned, hydrogen atoms were added, 4EI4 and 4L01 were added, and missing side chains were optimised. The prepared protein was subsequently used for receptor grid generation and docking simulations.

The network pharmacology studies illustrates of protein were made to identify the network signalling hub of the pathways. The PPI network data are mentioned in supplementary figure 1.

Figure 2. 3D representation of the (A) JAK1 protein with kinase activity of PDB ID: 4EI4; (B) JAK1 protein with pseudokinase activity of PDB ID: 4L01

2.3. Protein Refinement and Structure Validation

The JAK1 protein with kinase activity of PDB ID: 4EI4; (B) JAK1 protein with pseudokinase activity of PDB ID: 4L01 proteins structure was refined using the Mod Refiner server for protein refinement (**https://zhanglab.ccmb.med.umich.edu/ModRefiner/**, (accessed on 11 August 2021)). The Ramachandran plot was used to validate and evaluate the refined protein structures of proteins, revealing that the energetically allowed protein structure of 4EI4 and 4L01 regions for backbone dihedral angles toward amino acid residues were found. RAMPLOT was used to build the plots.

2.4. Molecular Docking Studies

The Pryx Version 0.8 open access docking software was used for the better understanding of molecular interaction and the docking between the JAK1 kinase domain (PDB ID: 4EI4), JAK1 pseudo kinase domain (PDB ID: 4L01) proteins and Pyrrolizidine (ligand) were uploaded. The grid box was marked to shield the active site residues, ready to be preferred binding residues to achieve the maximum orientation with the lowest binding affinity (Kcal/mol) values.

2.5. Molecular Dynamic Simulations

The compound (ligand) was initially filtered based on parameters including Glide score (Kcal/mol), non-bonded protein–ligand interactions, complementarity within the active site, and supporting evidence from existing literature. From this selection process, the most promising complex was subjected to molecular dynamics (MD) simulations using the Desmond module incorporated in the Schrödinger Suite 2022-23 (26). These simulations were conducted to assess the stability of the protein–ligand complex and its intermolecular interactions over time. For system preparation, the TIP3P water model was applied within an orthorhombic simulation box, and counter ions were introduced to achieve system neutrality. The finalised model was then imported into the molecular dynamics work panel, with the simulation executed for 200 ns. Following completion, trajectory analyses were performed through the Simulation Interaction Diagram tool available in the Desmond module (27).

RESULTS

3.1 Ramachandran Plot for JAK 1 (4EI4)

The Ramachandran analysis of **JAK1 (PDB ID: 4EI4)** demonstrated excellent stereochemical quality, with ≥99% of residues located within the allowed regions. Both 2D and 3D plots confirmed the protein's structural stability and integrity. The 2D plot revealed that most residues occupied the favored α-helical and β-sheet regions, while glycine exhibited broader angular dispersion due to its flexibility, and proline showed restricted φ/ψ distributions reflecting conformational constraints. The absence of residues in disallowed regions indicates high structural quality. The 3D Ramachandran plot further highlighted densely populated α-helical and β-sheet conformations through residue density peaks, confirming the dominance of stable secondary structures.

The detailed percentage values of allowed regions using Ramachandran plot has been mentioned in Supplementary figure 2 and 3. The secondary structure profiling of bothe the proteins mentions defines the α-helices and β-sheets regions of the protein, this values and results are mentioned in Supplementary figure 4 and 5

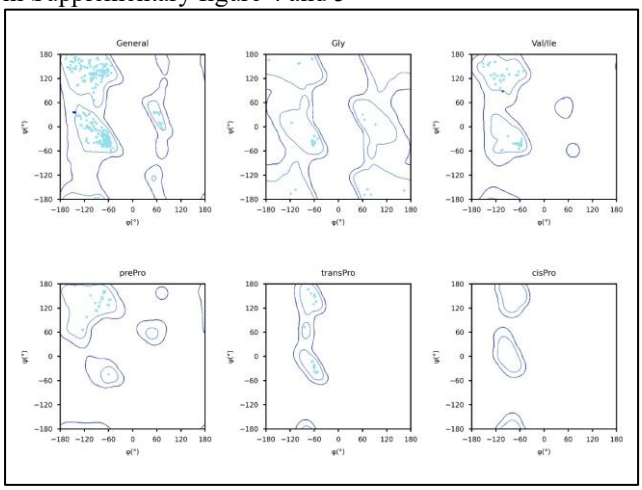

Figure 4a. 2D Ramachandran plots showing the distribution of φ (phi) and ψ (psi) dihedral angles for different residue categories: General, Glycine (Gly), Valine/Isoleucine (Val/Ile), pre-Proline (prePro), trans-Proline (transPro), and cis-Proline (cisPro). Contour regions represent allowed conformational space for each residue type.

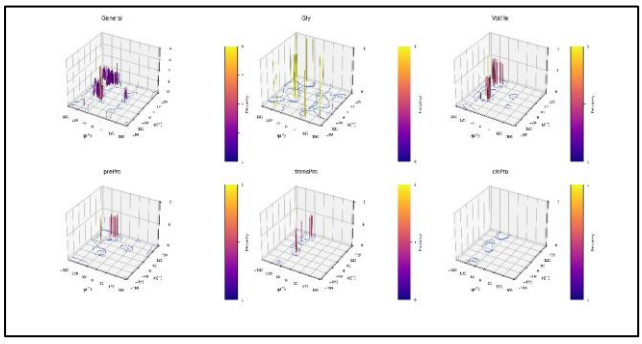

Figure 4b. 3D Ramachandran plots depicting the φ (phi) and ψ (psi) dihedral angle distributions for different residue categories: General, Glycine (Gly), Valine/Isoleucine (Val/Ile), pre-Proline (prePro), trans-Proline (transPro), and cis-Proline (cisPro). Colour

gradients indicate density of conformational states, with higher peaks representing more favorable regions

Similarly, the Ramachandran analysis of **Pseudo Kinase 1 (PDB ID: 4L01)** showed ≥99% of residues in allowed regions, indicating excellent stereochemical quality and structural integrity. The 2D plot depicted residues predominantly in favored regions corresponding to α-helices and β-sheets, with glycine and proline displaying their characteristic flexibility and conformational restrictions. The 3D plot provided additional insight into residue density distributions, revealing pronounced peaks corresponding to helix-rich regions, further supporting the protein's conformational stability and well-defined secondary structure organization.

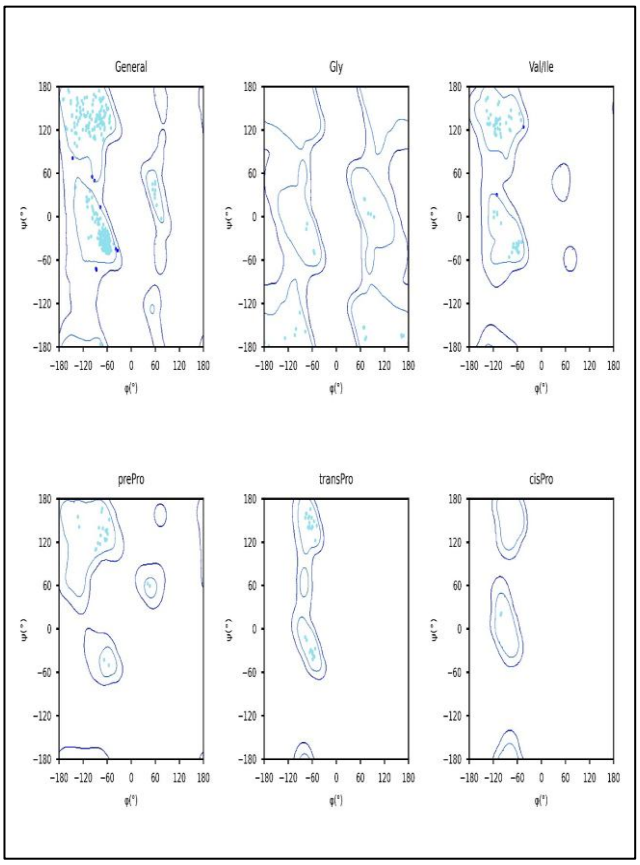

Figure 5a. 2D Ramachandran. The distribution of backbone dihedral angles (ϕ,ψ) for distinct residue types has been illustrated through Ramachandran plots. Data points corresponding to each residue type were analysed and represented as density contours to delineate regions of preferred conformational space. Separate panels have been presented for general amino acids, glycine, valine/isoleucine, pre-proline, trans-proline, and cis-proline, thereby demonstrating the unique steric and conformational preferences associated with each category. These plots were generated to facilitate comparative evaluation of allowed and disallowed regions for backbone torsion angles across different residue contexts.

Figure 5b. The image depicts three-dimensional surface plots representing the frequency distribution of backbone dihedral angles (ϕ, ψ) for six amino acid residue categories. For each group, general glycine, valine/isoleucine, pre-proline, trans-proline, and cis-proline, the 3D structure was indicated by vertical peaks rising from contour maps, where the height and colour intensity correspond to observed conformational density. These plots allow visualisation of sterically permitted and energetically favoured regions in 3D space, thus facilitating the assessment of structural propensities for each residue type. The applied visualisation method was intended to provide a comprehensive structural overview, with distinct conformational preferences clearly indicated for each amino acid context.

3.3 Molecular Docking Analysis and Visulaization

The molecular docking analysis revealed that the ligand exhibited the most favorable binding affinity toward **JAK1 with kinase activity** (−11.0 kcal/mol), compared to **JAK1 without kinase activity** (−8.4 kcal/mol). The interaction profile demonstrated multiple stabilizing polar contacts contributing to the enhanced binding stability. The ligand's structural features, including bulky *tert*-butyl substituents and fused *indan* and *pyrrolizine* cores, facilitated strong binding through a synergistic combination of polar interactions and hydrophobic packing within the proteins active site (Figures 6 and 7)

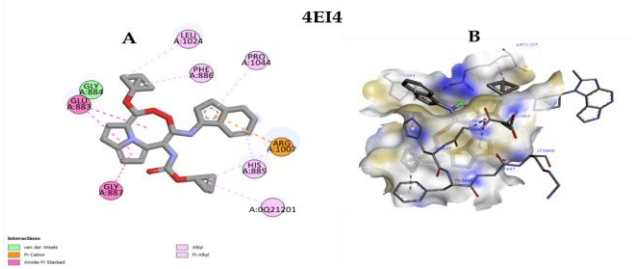

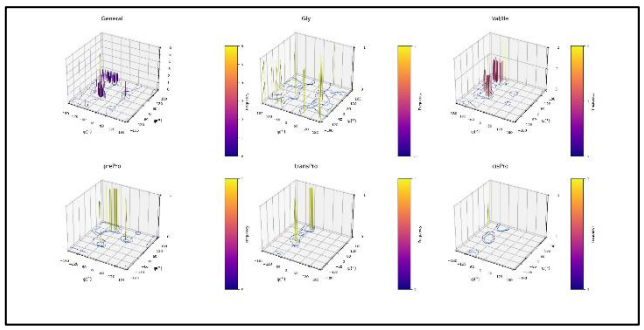

Figure 6. The figure (A) shows the 2D Structure of the ligand within the active site of the protein. The ligand forms a hydrogen bond with Arg1007(A) (green dashed line, 3.00 Å) and hydrophobic contacts with residues. These interactions collectively stabilise the ligand in the binding pocket. (B) Represents the 3D Structure of Protein-Ligand

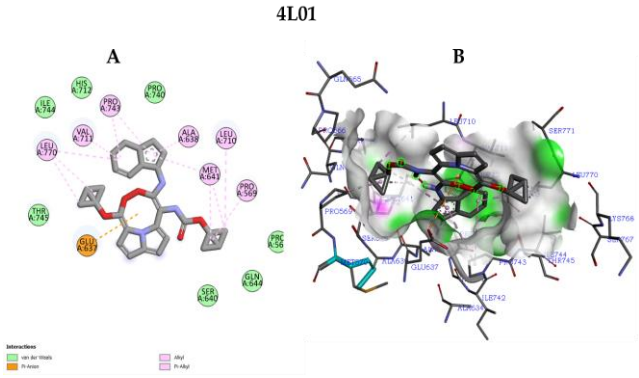

Figure 7. (A) The image displays a two-dimensional interaction diagram. The ligand is the black–blue–red molecular structure at the centre. Based on the visualisation, it appears to be a heterocyclic compound with multiple nitrogen atoms (blue), oxygen atoms (red), and fused aromatic rings. (B) Illustrating the binding interactions between a ligand and the surrounding amino acid residues within a protein active site. Various types of molecular contacts, including hydrogen bonds and hydrophobic interactions, are depicted through colour-coded dashed lines, with each interacting residue clearly labelled. This schematic representation facilitates the identification of key residues involved in ligand stabilisation and binding specificity.

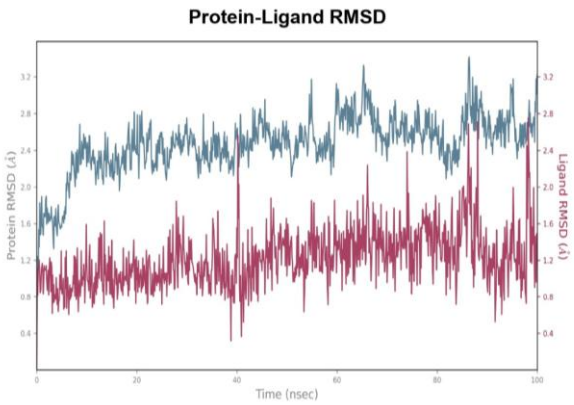

Figure 8 . Protein–ligand RMSD plot over a 100 ns molecular dynamics simulation. The protein backbone RMSD (blue) stabilizes around 2.4–2.8 Å after 20 ns, indicating structural equilibration. The ligand RMSD (red) remains consistently below 1.5 Å, suggesting stable binding of the ligand within the active site throughout the simulation.

3.4 Molecular Dynamics Simulation Results

A molecular dynamics (MD) simulation study was carried out to assess the stability of the receptor–ligand complex, verify the predicted binding conformation, and explore possible molecular interactions. These parameters had initially been analysed using Glide XP docking, and the current work further validated them through MD simulations**.** We ran for 100ns simulation of the Pyrrolizidine Derivative JAK 1complex.

3.4.1 Protein-Ligand RMSD

The Root Mean Square Deviation (RMSD) is used to measure the average change in displacement of a selection of atoms for a particular frame with respect to a reference frame. It is calculated for all frames in the trajectory. The procedure is repeated for every frame in the simulation trajectory.

The protein RMSD plot shows the RMSD evolution of a protein (left Y-axis). All protein frames are first aligned on the reference frame backbone, and then the RMSD is calculated based on the atom selection. Monitoring the RMSD of the protein can give insights into its structural conformation throughout the simulation. RMSD analysis can indicate if the simulation has equilibrated its fluctuations towards the end of the simulation, which are around some thermal average structure. Changes of the order of 1-3 Å are perfectly acceptable for small, globular proteins. Changes much larger than that, however, indicate that the protein is undergoing a large conformational change during the simulation. The RMSD values stabilise around a fixed value

Ligand RMSD (right Y-axis) indicates how stable the ligand is with respect to the protein and its binding pocket. In the above plot, 'Lig fit Prot' shows the RMSD of a ligand when the protein-ligand complex is first aligned on the protein backbone of the reference, and then the RMSD of the ligand heavy atoms is measured. The values observed are significantly larger than the RMSD of the protein, so the ligand has likely diffused away from its initial binding site, as shown in Figure 6.

3.4.2 Protein RMSF

The Root Mean Square Fluctuation (RMSF) is useful for characterising local changes along the protein chain. The plot below shows peaks that indicate areas of the protein that fluctuate the most during the simulation. Typically, it is observed that the tails (N- and C-terminal) fluctuate more than any other part of the protein. Secondary structure elements like alpha helices and beta strands are usually more rigid than the unstructured part of the protein, and thus fluctuate less than the loop regions, as shown in Figure 9

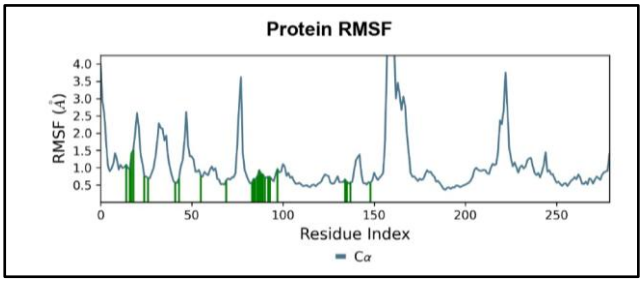

Figure 9. Protein RMSF (Root Mean Square Fluctuation) plot showing residue-wise flexibility of the Cα atoms during the molecular dynamics simulation. Peaks represent regions of higher flexibility, typically corresponding to loop regions, while lower RMSF values indicate more stable, structured areas. Green bars highlight residues involved in ligand interactions.

DISCUSSION

In the present investigation, a comprehensive molecular docking study was conducted to compare the binding affinity and interaction profile of a substituted pyrrolizidine derivative against the catalytic kinase domain (PDB ID: 4EI4) and the corresponding pseudokinase domain (PDB ID: 4L01) of Janus kinase 1 (JAK1). Before docking, rigorous structural validation of both protein targets was performed to ensure their stereochemical integrity and suitability for computational analysis. Ramachandran plot assessments demonstrated that more than 99% of amino acid residues for each domain were localised within energetically favourable regions, thereby confirming the high-quality geometry, minimised steric clashes, and appropriate backbone conformations of the selected crystal structures. This validation established a robust foundation for reliable docking and interaction analysis.

The architectural organisation of the JAK1 domains revealed the characteristic bilobal topology that is typical of protein kinases. Both the kinase and pseudokinase domains displayed a predominance of α-helical structures interspersed with β-sheets and flexible coil regions, forming the canonical N-lobe and C-lobe configuration. Such an organization facilitates ATP and ligand binding through the conserved hinge region, which often contributes key hydrogen-bonding residues essential for high-affinity interactions. These structural insights are crucial for understanding the conformational determinants governing ligand accommodation and specificity within the JAK family.

Ligand preparation involved energy minimisation and optimisation of the pyrrolizidine derivative to ensure geometrical stability and accurate charge distribution before docking. Receptor grid generation for each protein was meticulously defined around the ATP-binding cleft to capture the most relevant binding interactions. Glide docking simulations were subsequently performed using standard precision (SP) and extra precision (XP) modes to achieve refined scoring and pose ranking. The docking results indicated that the pyrrolizidine derivative exhibited stable binding orientations within the ATP-binding pockets of both domains, primarily stabilised by hydrogen bonding, π–π stacking, and hydrophobic interactions.

A comparative analysis of docking scores revealed that the kinase domain of JAK1 (4EI4) displayed a significantly stronger binding affinity, with a top-ranked docking score of –11.0 kcal/mol. The ligand formed three prominent hydrogen bonds with key residues within the hinge region, suggesting specific and stable engagement with catalytically relevant amino acids. In contrast, the pseudokinase domain (4L01) demonstrated a weaker interaction profile, characterised by a less negative docking score of –8.4 kcal/mol, despite forming a comparable number of hydrogen bonds. This difference likely reflects the diminished catalytic and structural flexibility of the pseudokinase domain, which lacks certain conserved residues critical for ATP binding and catalysis, thereby reducing its ability to accommodate the ligand in an energetically optimal configuration.

Collectively, these findings indicate that the kinase domain of JAK1 provides a more favourable binding environment for the substituted pyrrolizidine derivative, owing to its well-defined ATP-binding cleft, conserved catalytic residues, and higher conformational adaptability. The superior docking affinity observed for the kinase domain underscores its greater potential as a therapeutic target site for small-molecule inhibition. Furthermore, these results suggest that pyrrolizidine-based scaffolds may serve as promising lead structures for the rational design of selective JAK1 inhibitors aimed at modulating aberrant signalling pathways implicated in hepatocellular carcinoma progression. The comparative docking outcomes strongly support the hypothesis that the catalytic kinase domain of JAK1 is a more suitable and energetically preferred target for pyrrolizidine-based inhibitors than its pseudokinase counterpart. The observed interaction stability, hydrogen-bonding pattern, and favourable docking energy collectively highlight the potential of this compound class as a basis for developing next-generation JAK1-targeted therapeutics for liver cancer intervention.

CONCLUSION

The comparative molecular docking analysis demonstrated that the substituted pyrrolizidine derivative exhibits a markedly higher binding affinity and superior interaction stability toward the catalytic kinase domain of JAK1 compared to its pseudokinase counterpart. The lower docking energy (–11.0 kcal/mol) and the presence of multiple stabilizing hydrogen bonds within the ATP-binding cleft indicate a strong and specific ligand–protein interaction. In contrast, the pseudokinase domain showed a comparatively weaker binding affinity (–8.4 kcal/mol), likely due to its restricted conformational flexibility and reduced compatibility for ligand accommodation. These results collectively establish that the active kinase domain of JAK1 serves as a more suitable and energetically favourable binding target, positioning the pyrrolizidine derivative as a promising lead scaffold for the development of selective JAK1 inhibitors.

Collectively, the present findings underscore the therapeutic potential of pyrrolizidine derivatives as selective modulators of JAK1 signalling in hepatocellular carcinoma (HCC). By attenuating aberrant JAK1 activity, such compounds could inhibit tumour proliferation and enhance apoptotic sensitivity, addressing an important therapeutic gap in HCC treatment. However, while these computational insights are encouraging, further validation through in vitro kinase inhibition assays, cytotoxicity studies in HCC cell lines, and in vivo xenograft experiments is essential to confirm their efficacy and safety. Additionally, rational structural optimisation of the pyrrolizidine scaffold may improve target selectivity and minimise off-target effects, paving the way for the rational design of potent and clinically relevant JAK1-targeted therapeutics.

REFERENCE

1. Bray, F., Laversanne, M., Sung, H., Ferlay, J., Siegel, R. L., Soerjomataram, I., & Jemal, A. (2024). Global cancer statistics 2022: GLOBOCAN estimates of incidence and mortality worldwide for 36 cancers in 185 countries. CA: a cancer journal for clinicians, 74(3), 229–263. https://doi.org/10.3322/caac.21834

2. Gowda, S. V., Kim, N. Y., Harsha, K. B., Gowda, D.,

Suresh, R. N., Deivasigamani, A., Mohan, C. D., Hui, K. M., Sethi, G., Ahn, K. S., & Rangappa, K. S. (2025). A new 1,2,3-triazole-indirubin hybrid suppresses tumor growth and pulmonary metastasis by mitigating the HGF/c-MET axis in hepatocellular carcinoma. Journal of advanced research, 73, 341–356. https://doi.org/10.1016/j.jare.2024.08.033

3. Mohan, C. D., Shanmugam, M. K., Gowda, S. G. S., Chinnathambi, A., Rangappa, K. S., & Sethi, G. (2024). c-MET pathway in human malignancies and its targeting by natural compounds for cancer therapy. Phytomedicine : international journal of phytotherapy and phytopharmacology, 128, 155379. https://doi.org/10.1016/j.phymed.2024.155379

4. Hu, Y., Dong, Z., & Liu, K. (2024). Unraveling the complexity of STAT3 in cancer: molecular understanding and drug discovery. Journal of experimental & clinical cancer research : CR, 43(1), 23. https://doi.org/10.1186/s13046-024-02949-5

5. Huang, B., Lang, X., & Li, X. (2022). The role of IL-6/JAK2/STAT3 signaling pathway in cancers. Frontiers in oncology, 12, 1023177. https://doi.org/10.3389/fonc.2022.1023177

6. Wang, H. Q., Man, Q. W., Huo, F. Y., Gao, X., Lin, H., Li, S. R., Wang, J., Su, F. C., Cai, L., Shi, Y., Liu, B., & Bu, L. L. (2022). STAT3 pathway in cancers: Past, present, and future. MedComm, 3(2), e124. https://doi.org/10.1002/mco2.124

7. Mohan, C. D., Bharathkumar, H., Bulusu, K. C., Pandey, V., Rangappa, S., Fuchs, J. E., Shanmugam, M. K., Dai, X., Li, F., Deivasigamani, A., Hui, K. M., Kumar, A. P., Lobie, P. E., Bender, A., Basappa, Sethi, G., & Rangappa, K. S. (2014). Development of a novel azaspirane that targets the Janus kinase-signal transducer and activator of transcription (STAT) pathway in hepatocellular carcinoma in vitro and in vivo. The Journal of biological chemistry, 289(49), 34296–34307. https://doi.org/10.1074/jbc.M114.601104

8. Manore, S. G., Doheny, D. L., Wong, G. L., & Lo, H. W. (2022). IL-6/JAK/STAT3 Signaling in Breast Cancer Metastasis: Biology and Treatment. Frontiers in oncology, 12, 866014. https://doi.org/10.3389/fonc.2022.866014

9. Mohan, C. D., Rangappa, S., Preetham, H. D., Chandra Nayaka, S., Gupta, V. K., Basappa, S., Sethi, G., & Rangappa, K. S. (2022). Targeting STAT3 signaling pathway in cancer by agents derived from Mother Nature. Seminars in cancer biology, 80, 157–182. https://doi.org/10.1016/j.semcancer.2020.03.016

10. Mohan, C. D., Rangappa, S., Nayak, S. C., Sethi, G., & Rangappa, K. S. (2021). Paradoxical functions of long noncoding RNAs in modulating STAT3 signaling pathway in hepatocellular carcinoma. Biochimica et biophysica acta. Reviews on cancer, 1876(1), 188574. https://doi.org/10.1016/j.bbcan.2021.188574

11. Zhou, Y., Wang, M., Qian, Y., Yu, D., Zhang, J., Fu, M., Zhang, X., Qin, R., Ji, R., Zhang, X., & Gu, J. (2025). PRDX2 promotes gastric cancer progression by forming a feedback loop with PKM2/STAT3 axis. Cellular signalling, 127, 111586. https://doi.org/10.1016/j.cellsig.2024.111586

12. Zhao, Z., Yu, P., Wang, Y., Li, H., Qiao, H., Sun, C., Zhu, L., & Yang, P. (2024). Silencing of STEAP3 suppresses cervical cancer cell proliferation and migration via JAK/STAT3 signaling pathway. Cancer & metabolism, 12(1), 40. https://doi.org/10.1186/s40170-024-00370-2

13. Gouda, A. M., Abdelazeem, A. H., Arafa, el-S. A., & Abdellatif, K. R. (2014). Design, synthesis and pharmacological evaluation of novel pyrrolizine derivatives as potential anticancer agents. Bioorganic chemistry, 53, 1–7. https://doi.org/10.1016/j.bioorg.2014.01.001

14. Belal A. (2015). Synthesis, molecular docking and antitumor activity of novel pyrrolizines with potential as EGFR-TK inhibitors. Bioorganic chemistry, 59, 124–129. https://doi.org/10.1016/j.bioorg.2015.02.006

15. Shawky, A. M., Ibrahim, N. A., Abourehab, M. A. S., Abdalla, A. N., & Gouda, A. M. (2021). Pharmacophore-based virtual screening, synthesis, biological evaluation, and molecular docking study of novel pyrrolizines bearing urea/thiourea moieties with potential cytotoxicity and CDK inhibitory activities. Journal of enzyme inhibition and medicinal chemistry, 36(1), 15–33. https://doi.org/10.1080/14756366.2020.1837124

16. Shawky, A. M., Abdalla, A. N., Ibrahim, N. A., Abourehab, M. A. S., & Gouda, A. M. (2021). Discovery of new pyrimidopyrrolizine/indolizine-based derivatives as P-glycoprotein inhibitors: Design, synthesis, cytotoxicity, and MDR reversal activities. European journal of medicinal chemistry, 218, 113403. https://doi.org/10.1016/j.ejmech.2021.113403

17. He, J., Zhang, W., Zheng, C., Qiu, Y., Zheng, W., Zhang, Q., … Xie, J. (2019). Title of the article. Bioorganic & Medicinal Chemistry Letters. https://doi.org/10.1016/j.bmcl.2019.04.008

18. Kumar, M., & Rathore, R. S. (2025). RamPlot: A webserver to draw 2D, 3D and assorted Ramachandran (φ, ψ) maps. Journal of Applied Crystallography, 58(3), 630-636. https://doi.org/10.1107/S1600576725001669

19. Ashok Kumar, T. (2013). CFSSP: Chou and Fasman Secondary Structure Prediction server. WIDE SPECTRUM: Research Journal. 1(9):15-19.

20. Friesner, R. A., Banks, J. L., Murphy, R. B., Halgren, T. A., Klicic, J. J., Mainz, D. T., … Shenkin, P. S. (2004). Glide: A new approach for rapid, accurate docking and scoring. Journal of Medicinal Chemistry, 47(7), 1739–1749. https://doi.org/10.1021/jm0306430 pubmed.ncbi.nlm.nih.gov

21. Ban, T. A., Sonawane, V. R., & Suresh, C. G. (2018). A multiple-grid arrangement method for receptor grid generation in docking using Glide. Computational Biology and Chemistry, 74, 56–63. https://doi.org/10.1016/j.compbiolchem.2018.02.012
22. Schrödinger, LLC. (2015). The PyMOL molecular graphics system (Version 1.8) [Computer software]. Schrödinger, LLC.
23. Schrödinger, LLC. (2021). LigPrep (Version 2021-4) [Computer software]. Schrödinger, LLC.
24. Schrödinger, LLC. (2021). Protein Preparation Wizard (Version 2021-4) [Computer software]. Schrödinger, LLC.
25. Schrödinger, LLC. (2021). Jaguar (Version 2021-4) [Computer software]. Schrödinger, LLC.
26. Schrödinger, LLC. (n.d.). Maestro [Computer software]. Retrieved from https://newsite.schrodinger.com/platform/products/maestro/
27. Niazi, S., Kavana, C. P., Aishwarya, H. K., Dharmashekar, C., Jain, A., Wani, T. A., Shivamallu, C., Purohit, M. N., & Kollur, S. P. (2024). Synthesis, characterization, and anti-cancer potential of novel p53-mediated Mdm2 and Pirh2 modulators: An integrated in silico and in vitro approach. Frontiers in Chemistry, 12, 1366370. https://doi.org/10.3389/fchem.2024.1366370
28. World Health Organization. (2022). Cancer fact sheet: Liver cancer. https://www.who.int/news-room/fact-sheets/detail/cancer
29. He, G., & Karin, M. (2011). NF-κB and STAT3 – Key players in liver inflammation and cancer. Cell Research, 21(1), 159–168. https://doi.org/10.1038/cr.2010.177
30. Wang, T., Niu, G., Kortylewski, M., Burdelya, L., Shain, K., Zhang, S., … Yu, H. (2004). Regulation of the innate and adaptive immune responses by Stat-3 signaling in tumor cells. Nature Medicine, 10(1), 48–54. https://doi.org/10.1038/nm974
31. Rawlings, J. S., Rosler, K. M., & Harrison, D. A. (2004). The JAK/STAT signaling pathway. Journal of Cell Science, 117(8), 1281–1283. https://doi.org/10.1242/jcs.00963
32. Kaur, S., Batra, S., & Batra, J. (2018). Targeting JAK/STAT pathway in cancer: A focus on hepatocellular carcinoma. OncoTargets and Therapy, 11, 3895–3908. https://doi.org/10.2147/OTT.S172585.
33. Haan, C., Rolvering, C., Raulf, F., Kapp, M., Drückes, P., Thoma, G., Behrmann, I., & Zerwes, H.-G. (2011). JAK1 has a dominant role over JAK3 in signal transduction through γc-containing cytokine receptors. FEBS Journal, 278(22), 3899–3911. https://doi.org/10.1111/j.1742-4658.2011.08349.x
34. Bopage, S. R., Pathirana, C., & Rathnayake, A. D. (2019). Pyrrolizidine alkaloids and their derivatives: Chemistry, biological activities, and medicinal applications. Bioorganic & Medicinal Chemistry Letters, 29(12), 1531–1544. https://doi.org/10.1016/j.bmcl.2019.04.008